Title

The mitochondrial chaperone Prohibitin 1 negatively regulates interleukin-8 in human liver cancers

Journal

Journal of Biological Chemistry, 294(6)

ISSN

0021-9258

Authors

Yang, Jin Won
Murray, Ben
Barbier-Torres, Lucia
et al.

Publication Date

2019-02-01

DOI

10.1074/jbc.ra118.004863

Peer reviewed

The mitochondrial chaperone Prohibitin 1 negatively regulates interleukin-8 in human liver cancers

Jin Won Yang[1,2*], Ben Murray[1*], Lucia Barbier-Torres[1*], Ting Liu[3], Zhenqiu Liu[4], Heping Yang[1], Wei Fan[1] Jiaohong Wang[1], Yuan Li[1,3], Ekihiro Seki[1], José M. Mato[5], and Shelly C. Lu[1]

From the [1]Division of Digestive and Liver Diseases, Cedars-Sinai Medical Center, LA, CA 90048, USA; [2]College of Pharmacy, Woosuk University, Wanju, South Korea; [3]Department of Gastroenterology, Xiangya Hospital, Central South University, Changsha, Hunan, China; [4]Department of Public Health Sciences, Penn State College of Medicine, Hershey, PA; [5]CIC bioGUNE, Centro de Investigación Biomédica en Red de Enfermedades Hepáticas y Digestivas (Ciberehd), Technology, Park of Bizkaia, 48160 Derio, Bizkaia, Spain

Running title: *Prohibitin 1 negatively regulates IL-8 transcription*

*Share first-authorship

To whom correspondence should be addressed: Shelly C. Lu, M.D., Cedars-Sinai Medical Center, Davis Building, Room #2097, 8700 Beverly Blvd., Los Angeles, CA, 90048. Tel: (310) 423-5692, Fax: (310) 423-0653, e-mail: shelly.lu@cshs.org

Keywords: Interleukin-8, Jun N-terminal Kinase, liver cancer, nuclear factor κB, prohibitin 1, tumor supressor

ABSTRACT

Prohibitin 1 (PHB1) is a mitochondrial chaperone whose expression is dysregulated in cancers. In liver cancer, PHB1 acts as a tumor suppressor but the mechanisms of tumor suppression are incompletely understood. Here we aimed to determine PHB1 target genes to better understand how PHB1 influences liver tumorigenesis. Using RNA-seq analysis, we found interleukin-8 (IL-8) to be one of the most highly upregulated genes following PHB1 silencing in HepG2 cells. Induction of IL-8 expression also occurred in multiple liver and non-liver cancer cell lines. We examined samples from 178 patients with hepatocellular carcinoma (HCC) and found that *IL-8* mRNA levels were increased, while *PHB1* mRNA levels were decreased, in the tumors compared to adjacent non-tumorous tissues. Notably, HCC patients with high IL-8 expression have significantly reduced survival. An inverse correlation between *PHB1* and *IL-8* mRNA levels is found in HCCs with reduced PHB1 expression. To understand the molecular basis for these observations, we altered PHB1 levels in liver cancer cells. Overexpression of PHB1 resulted in lowered IL-8 expression and secretion. Silencing PHB1 increased JNK and NF-κB activity, induced nuclear accumulation of c-JUN and p65 and enhanced their binding to the *IL-8* promoter containing AP-1 and NF-κB elements. Conditioned medium from PHB1-silenced HepG2 cells increased migration and invasion of parental HepG2 and SK-hep-1 cells, and this was blocked by co-treatment with neutralizing IL-8 antibody. In summary, our findings show that reduced PHB1 expression induces *IL-8* transcription by activating NF-κB and AP-1, resulting in enhanced IL-8 expression and release to promote tumorigenesis.

Prohibitin 1 (PHB1) is a highly conserved, ubiquitously expressed protein with diverse functions located in multiple cellular compartments. PHB1 was first identified as a mitochondrial chaperone that is essential for function and biogenesis of the mitochondria (1). Nuclear PHB1 interacts with many proteins including retinoblastoma and p53, where it serves as a transcriptional cofactor repressing or activating the transcriptional activities of E2F (2, 3) or p53

(4), respectively. PHB1 was thought to act as a tumor suppressor because its expression was suppressed after partial hepatectomy prior to liver regeneration (5). However, the role of PHB1 in cancer remains controversial since PHB1 is overexpressed in some cancers (6). Nevertheless, PHB1 has a clearly tumor suppressive role in breast, gastric, and prostate cancers (7, 8). In addition, reduced PHB1 expression occurs in patients with inflammatory bowel disease, a chronic inflammatory condition that predisposes to colon cancer, and overexpression of PHB1 inhibits colitis-associated colon cancer tumorigenesis in mice (9).

Our group reported that hepatic PHB1 expression is reduced during chronic cholestatic injury in both experimental murine models and in humans (10, 11). We also reported that liver-specific *Phb1* knockout (KO) mice develop hepatocellular carcinoma (HCC) (12) and *Phb1* heterozygotes are predisposed to cholestasis-associated cholangiocarcinoma (CCA) (13). We found that hepatic PHB1 expression is down-regulated at the mRNA level in the majority of human patients with HCC and CCA, and reduced PHB1 expression increases the growth of HCC and CCA cells and inversely correlates with tumor growth in the murine CCA model (13). We have identified two potential mechanisms of PHB1's tumor suppressive effects in the liver; first is by negatively regulating the insulin-like growth factor 2 (IGF2)-H19 axis (14) and second is to heterodimerize with MAX to bind and repress E-box driven gene expression, such as c-MYC (13). A major goal of this work was to identify other targets of PHB1 that are important in liver tumorigenesis.

In the course of our investigation we uncovered the finding that PHB1 negatively regulates the expression of the pro-tumorigenic interleukin 8 (IL-8) at the transcriptional level. Loss of PHB1 in multiple cancer cell lines increases the expression of IL-8, which in turn increases the migration and invasion properties of these cells. Our findings are confirmed in human HCC samples and suggest that PHB1 plays an important role in suppressing the development of liver cancers by multiple mechanisms.

RESULTS

PHB1 silencing in liver and colon cancer cell lines upregulates cancer genes

To identify PHB1-regulated genes, PHB1 was silenced in HepG2 cells and then subjected to RNA-Sequencing. Seventy two hours silencing of PHB1 was required to achieve efficient knockdown at the protein level and no effect was observed on cell viability at this time (Supplemental Fig. 1A-B). After pathway enrichment analysis, genes related to cancers were the most highly altered (4.54% of genes) (Fig. 1A). Examining the upregulated genes in the cancer pathways revealed that *IL-8*, platelet-derived growth factor subunit A (*PDGFA*), matrix metalloproteinase-2 (*MMP2*), and transforming growth factor beta-1 (*TGFB1*) were highly upregulated (Fig. 1B). These findings were confirmed using real-time PCR in HepG2 cells after 72 hours of PHB1 silencing (Fig. 1C). We focused our efforts on IL-8, as it is the most upregulated gene in the cancer pathways. Silencing PHB1 also raised *IL-8* mRNA levels in multiple cancer cell lines of different sources, including HCT116 (colorectal carcinoma), Huh7 (HCC), and Mz-ChA1 (biliary adenocarcinoma) (Fig. 1D).

Increased IL-8 levels in HCC correlates with poorer patient outcome

To assess the clinical relevance of PHB1 and IL-8 in HCC, the mRNA levels of *PHB1* and *IL-8* in 178 patients with HCC were measured. *PHB1* mRNA levels were lower in HCC as compared to adjacent non-tumorous tissue whilst *IL-8* mRNA levels were higher (Fig. 2A). However, there is no correlation between *PHB1* and *IL-8* mRNA levels when all of the HCC samples were analyzed ($P = 0.22$) (data not shown). Since the patient samples are likely to be highly heterogeneous, we clustered the patients into three subgroups (subtypes): Cluster I with elevated *PHB1* but lower *IL-8* mRNA levels as compared to adjacent NT (58 of 178 patients), cluster II with the reduced expression of PHB1 (91 of 178 patients with *PHB1* mRNA levels = 28±2% of adjacent NT), and cluster III with higher *PHB1* and *IL-8* mRNA levels as compared to adjacent NT (29 of 178 patients) as shown in Figure 2B. We examined the correlations between PHB1 and IL-8 expression in each patient subgroup and detected a significant negative correlation between *PHB1* and *IL-8* mRNA levels in cluster II ($P = 0.02$) where HCC PHB1 expression is reduced,

as shown in Figure 2C. *IL-8* mRNA levels were also elevated compared to adjacent normal samples in multiple gene expression omnibus datasets of HCC (Fig. 2D). Poor patient outcome also correlated with higher *IL-8* mRNA levels as low levels had 60% chance of survival after 2,500 days as compared to 20% chance of survival in patients with high levels (Fig. 2E).

Loss of PHB1 increases levels of intracellular and secreted IL-8 in liver cancer cells

As IL-8 is a cytokine that is secreted from the cell to exert autocrine and paracrine effects on neighboring cells, we examined levels of this protein upon silencing of PHB1 in several liver cancer cell lines. Silencing PHB1 caused an increase in both the intracellular and secreted protein levels of IL-8 as compared to the scramble siRNA control in HepG2, Huh7 and Hep3B cell lines (Fig. 3A, and second siRNA shown in Supplemental Figure 1C). Conversely when PHB1 was overexpressed in Huh7 and Hep3B cells, *IL-8* mRNA levels fell by 50-60% (Fig. 3B) whilst intracellular IL-8 protein levels dropped by 75% (Fig. 3C). A significant drop in secreted IL-8 protein (>50%) was also observed in both liver cancer cell lines (Fig. 3C). Overexpression of PHB1 was not explored in HepG2 cells as basal IL-8 expression is very low (Fig. 3A).

PHB1 silencing mediated increase in IL-8 levels is c-JUN N-terminal kinase (JNK) and nuclear factor-κB (NF-κB) dependent

Previous studies have shown p38 can regulate *IL-8* mRNA stability whilst JNK, NF-κB, and extracellular signal-regulated kinase (ERK) can transcriptionally regulate IL-8 (15-17). Silencing of PHB1 showed no effect on *IL-8* mRNA stability (Fig. 4A). Silencing PHB1 in HepG2 cells resulted in a marked increase in the levels of phosphorylated JNK (p-JNK) and p38 (p-p38), but a slight increase in total JNK while total p38 was unchanged. This led to a dramatic increase in the p-JNK:JNK and p-p38:p38 ratios (Fig. 4B). Both p-ERK and total ERK levels showed a slight increase, so that p-ERK:ERK was unchanged (Fig. 4B). To see if PHB1 silencing mediated increase in IL-8 expression was due to known IL-8 regulators, inhibitors against p38, NF-κB and JNK were used in combination with PHB1 silencing to see the effect on *IL-8* mRNA levels. The use of any of the inhibitors had no effect on *IL-8* mRNA levels when PHB1 was present. Upon PHB1 silencing, *IL-8* mRNA levels increased 9-fold, which was unaffected by the p38 inhibitor, SB (Supplemental Figure 1D). However, when either of the inhibitors against NF-κB (JSH) or JNK (SP) was used, the IL-8 induction due to PHB1 silencing was reduced by 40% but combining JSH with SP resulted in a near complete inhibition of IL-8 induction (Fig. 4C). This supports the effect of PHB1 silencing on IL-8 induction is mediated via JNK and NF-κB.

PHB1 silencing induces the human IL-8 promoter activity via NF-κB and AP-1 sites

To further elucidate JNK and NF-κB's roles in the upregulation of IL-8, promoter luciferase reporter constructs of human IL-8 were created. The human *IL-8* promoter contains both NF-κB and AP-1 binding sites. Upon silencing of PHB1 the promoter activity of both NF-κB and AP-1 increased 6- and 4-fold, respectively (Fig. 5A). To define which binding sites was involved in the induction of IL-8 expression, HepG2 cells were transfected with PHB1 siRNA and the effects on the full-length *IL-8* promoter (-1450/+154) or a shorter construct *IL-8*-promoter (-162/+44) that was wild type (WT) or mutated in the AP-1 or NF-κB elements were measured. The full length construct (-1450/+154) and the shorter WT construct (-162/+44) showed comparable increase in promoter activity when PHB1 was silenced, suggesting the -162/+44 construct contains all essential elements that mediate this induction (Fig. 5B). However, the basal activity was reduced when the AP-1 binding site was mutated and was completely abolished upon mutation of the NF-κB site (Fig 5B). Silencing PHB1 failed to increase the *IL-8* promoter activity when either the AP-1 or NF-κB site was mutated (Fig. 5B). To confirm the importance of NF-κB and AP-1, the levels of the p65 and c-JUN were examined in the nuclear fraction of HepG2 cells afer PHB1 silencing. A 6-fold increase in c-JUN level was observed in PHB1 silenced cells as well as a 2-fold increase in p65 level (Fig. 5C). ChIP-qPCR also confirmed the increase of both p65 and c-JUN binding to the *IL-8* promoter when PHB1 was silenced (Fig 5D). Elevation in nuclear p65 level is a result of canonical NF-κB activation, as shown by early phosphorylation of IκB kinase (IKK) and IκBα at 24 hours after silencing PHB1, followed by a drop in IκBα protein level at 48-72 hours (Fig. 5E).

Since PHB1 can act as a transcription co-factor to modulate the activity of p53, E2F and c-MYC (2, 3, 13), we examined whether it can bind to the IL-8 promoter region containing the AP-1 and NF-κB elements using ChIP and sequential-ChIP (Fig. 6A). We found that PHB1 is unable to bind to the DNA by itself (Fig. 6B), or in the presence of p50, p65 or c-FOS (Fig. 6C-E), but it was able to bind in the presence of c-JUN (Fig. 6F). This raises the possibility that PHB1 could also act as a co-repressor of the AP-1 site.

Mechanisms of PHB1 silencing-induced activation of JNK and NF-κB

Since PHB1 is a well-known mitochondrial chaperone, we next investigated whether mitochondrial dysfunction and increased reactive oxygen species (ROS) could be the underlying mechanism for activation of JNK and NF-κB. Mitochondrial membrane potential and both mitochondrial and total ROS were measured following 48 and 72 hours of treatment with PHB1 siRNA or scramble control and no significant change was observed in these variables (Supplemental Fig. 2A-C). Another possibility is transforming growth factor beta-activated kinase 1 (TAK1), which is known to activate JNK, p38 and NF-κB (18). However, PHB1 silencing did not activate TAK1 (indicated by p-TAK1), which was only detectable in the presence of calyculin A (Supplemental Fig. 2D) (19).

Blocking PHB1 knockdown-induced IL-8 secretion prevents migration and invasion of liver cancer cells

Previous work has shown that IL-8 production from cancer cells increases the migration of adjacent cells (20). To explore whether silencing of PHB1 could affect the migration of parental cells, conditioned medium (CM) from PHB1 silenced-HepG2 cells was used on HepG2, a non-invasive epithelial cell line, and SK-hep-1 cells, a highly invasive human hepatic adenocarcinoma cell line with oncogenic mesenchymal stem cell features (21). Both cell lines observed an increase in cell migration using CM from PHB1 silenced HepG2 cells as compared to the scramble control, which was significantly attenuated or inhibited when co-treated with a neutralizing IL-8 antibody (Fig. 7A-B). Furthermore, the effects of CM on invasion in SK-hep-1 cells was examined and CM from PHB1 silenced HepG2 cells increased cell invasion, which was attenuated upon co-treatment with the neutralizing IL-8 antibody (Fig. 7C).

DISCUSSION

Although PHB1 is best known as a mitochondrial chaperone protein, increasing evidence shows it has many other important functions, some of which pertain to cancer. Subcellular localization and post-translational modifications may explain the tumor regulatory activity of PHB1 in different cell types (14, 22). In particular, mitochondrial and membrane-associated PHB1 in some cancer cells (such as cervical, lung and bladder) have been shown to confer anti-apoptotic effects and tumorigenesis (23-25). In contrast, nuclear PHB1 exhibits pro-apoptotic or anti-tumorigenic properties. In breast, prostate, osteosarcoma and colon cancer cells, PHB1 is mainly localized in the nucleus and PHB1 sliencing increased cell proliferation (4, 26-29). We also found that PHB1 is mainly localized in the nucleus in three different HCC cell types including HepG2, Huh7 and Hep3B cancer cell lines (Supplemental Fig. 3). This may be part of the explanation why PHB1 appear to act mainly as a tumor suppressor in the liver (12-14). In the nucleus PHB1 acts as a transcription co-factor that can either activate (such as p53) or repress (such as E2F1) gene expression (2-4). We have described in liver cancer cells two other tumor suppressive mechanisms, including PHB1 acting as a co-repressor with CCCT-binding transcription factor CTCF on the imprinting control region to suppress IGF2-H19 (14), and as a heterodimer with MAX to repress E-box-dependent genes, such as c-MYC and MAFG, both oncogenes in the liver (13, 30). In the present work we uncovered additional signaling pathways that are regulated by PHB1 that also affect gene expression, in this case IL-8, that can contribute to tumorigenesis, invasion and metastasis when PHB1 expression is lost.

Proinflammatory cytokines play an important role in tumor progression and metastatsis as they are mediators of the paracrine signal between both the tumor and the tumor microenvironment (31). IL-8 is a multifunctional CXC chemokine as well as a proinflammatory cytokine that promotes neutrophil chemotaxis and activation (32). IL-8 is produced in the both tumor cells and tumor-associated macrophages and plays a critical role in

cancer-related inflammation by promoting invasion and metastasis in human cancers (33). Importantly, IL-8 has been reported to be overexpressed and associated with high recurrence rates and short survival in the patients with HCC and its upregulation promoted HCC invasion and metastasis (34, 35). We identified IL-8 as one of the most upregulated genes when PHB1 was silenced in HepG2 cells on RNA sequencing and confirmed that this also occurs in multiple other liver cancer cell lines as well as in HCT116, a colon cancer cell line where PHB1 also behaves as a tumor suppressor (Fig. 1D) (29). Silencing PHB1 raised, while overexpressing PHB1 lowered intracellular and secreted IL-8 levels in liver cancer cells (Fig. 3). We also confirmed that high IL-8 expression occurs in most human HCC, is associated with worse survival, and is inversely associated with PHB1 in a subgroup of patients where PHB1 expression is reduced (Fig. 2). At the present time the mechanisms for heterogenous expression of PHB1 in HCC remains unexplained and will be a focus of future study.

We next focused on elucidating how PHB1 negatively regulates IL-8 at the mRNA level. Increased IL-8 expression can be mediated by the activation of the MAP kinases ERK, JNK, and p38 as well as NF-κB activation (15-17). JNK activation has been shown to be essential for IL-8 expression through c-JUN (36). p38 activation has been shown to stabilize IL-8 mRNA in HeLa cells (17). We were unable to find any literature on the direct regulation of p38 or JNK by PHB1, although an increase in JNK activity has been observed in *Phb1*-KO livers after bile-duct ligation that was attributed to increased ROS (11). It has been described previously that PHB1 regulates NF-κB nuclear translocation by decreasing importin α3 expression (37). This is consistant with our results whereby PHB1 silencing increases the nuclear content of p65 (Fig. 5C). However, we found PHB1 silencing turned on the canonical NF-κB activation pathway (Fig. 5E), suggesting more than one mechanism may be involved in elevating nuclear p65 level. Available literature suggest PHB1 positively regulates ERK activity in HeLa cells (38) and rat granulosa cells (39). However, in liver cancer cells PHB1 silencing had no effect on ERK activity.

Our study showed that in liver cancer cells PHB1 silencing activated JNK, p38, and NF-κB. Inhibition of JNK strongly attenuated the ability of PHB1 silencing-mediated IL-8 induction but inhibition of p38 had no effect (Fig. 4). Consistently, PHB1 silencing did not influence *IL-8* mRNA stabilization. In addition, inhibiting NF-κB also attenuated IL-8 induction (Fig. 4). When both JNK and NF-κB were inhibited, PHB1 silencing no longer induced IL-8 expression (Fig. 4C). Taken together, our results show PHB1 silencing increased IL-8 expression at the transcription level by mechanisms that require JNK and NF-κB.

Transcritional regulation of human *IL-8* is mainly by NF-κB and AP-1. The region from +1 to -133 within the 5′-flanking region of the human *IL-8* promoter is critical for the transcriptional regulation of *IL-8* (40) and contains the binding sites for NF-κB and AP-1. We found the activity of the construct −162/44-Luc was very similar to the activity of −1450/154-Luc, suggesting that all the important elements are contained within −162/44 of the human *IL-8* promoter. Consistently, mutation of the AP-1 site lowered the basal promoter activity and prevented *IL-8* promoter activation by PHB1 silencing. On the other hand, mutation of the NF-κB site abolished both basal and PHB1 silencing-induced promoter activity. This result suggests that NF-κB site is essential for the basal activity of *IL-8* promoter and both AP-1 and NF-κB are required for PHB1 silencing to activate the *IL-8* promoter. Indeed, PHB1 silencing activated reporter activity driven by both AP-1 and NF-κB elements, nuclear accumulation of c-JUN and p65 and their binding to the *IL-8* promoter (Fig. 5). In addition, we found PHB1 was able to bind to the IL-8 promoter region in the presence of c-JUN (Fig. 6F), which raises the possibility that PHB1 can also serve as a co-repressor of the AP-1 site.

JNK, p38 and NF-κB are all known to be regulated by oxidative stress, which prompted us to speculate whether silencing PHB1 could have led to mitochondrial dysfunction and increased ROS. However, there was no evidence for increased ROS or mitochondrial dysfunction under the experiment conditions (Supplemental Fig. 2A-C). This was somewhat surprising since PHB1 is a well-known mitochondrial chaperone. One possibility may have to do with where PHB1 is mainly localized in the cell under study. The three cell lines we used all seem to have a predominance of PHB1 in the nuclear compartment (Supplemental Fig. 3), where

it may play more of a tumor suppressor role. Thus, increased ROS is not the underlying mechanism for activation of JNK, p38 and NF-κB. Another potential mechanism is TAK1, which has an important role in the regulation of inflammatory disorders including cancer and regulates IL-8 expression through AP-1 and NF-κB pathway (19, 40). However, PHB1 silencing did not affect TAK1 activation (Supplemental Fig. 2D). Since p-TAK1 was only detectable when cells were treated with calyculin A to block its dephosphorylation (19) it is possible that we may have missed a small upregulation that was masked by calyculin A. The underlying molecular mechanisms of how PHB1 regulates JNK and p38 remain unclear and will require further investigation.

Tumor-derived IL-8 has been shown to promote the invasion and migration of adjacent tumor cells (41). We also found conditioned medium from PHB1-silenced HepG2 cells induced migration and invasion of parental HepG2 cells and SK-hep-1 cells, the latter is a highly invasive cell line that has a more mesenchymal feature. Both migration and invasion were significantly attenuated in the presence of neutralizing antibody to IL-8 (Fig. 7), which illustrates one mechanism for PHB1 loss to promote a more aggressive liver cancer phenotype is through upregulation and release of IL-8.

In summary, we have identified a novel mechanism by which reduced PHB1 expression increased *IL-8* transcription by activating NF-κB and JNK/AP-1 pathways. Loss of PHB1 leads to increased release of IL-8, which can stimulate cancer cell migration and invasion in autocrine and paracrine manner. Our findings provide further insight into the molecular mechanisms of IL-8 regulation and added JNK, p38 and NF-κB signaling pathways that are normally suppressed by PHB1 in liver cancer cells.

EXPERIMENTAL PROCEDURES

Source of human HCC with adjacent non-tumorous specimens

178 HCC specimens and adjacent non-tumorous tissues were obtained from Xiangya Hospital Central South University, Changsha, Hunan province, China. These specimens were fresh-frozen samples obtained from patients undergoing surgical liver resection from 2013 to 2017 and were stored in liquid nitrogen in the institutional biobank. All human specimens were obtained with patients' informed consent. The use of human samples was approved by the Institutional Review Board of the Central South University, Xiangya Hospital Authority. The study protocol conformed to the ethical guidelines of the 1975 Declaration of Helsinki as reflected in *a priori* approval by the Institutional Review Boards of the Medical Ethical Committee of Xiangya Hospital Central South University.

TCGA dataset from OncoLnc

Graph showing survival analysis was generated using TCGA dataset from OncoLnc (http://www.oncolnc.org/) (41, 42).

Cell culture and treatments with inhibitors of p38, NF-κB and JNK

Human CCA MzChA-1 and HCC HepG2, Hep3B and Huh7 cell lines were cultured in DMEM supplemented with 10% fetal bovine serum (FBS), 100 U/mL penicillin, 0.1 mg/mL streptomycin, and 2 mmol/L L-glutamine. Human colorectal adenocarcinoma HCT116 cell line was cultured in McCoy's 5A media containing 10% FBS, 100 U/mL penicillin, 0.1 mg/mL streptomycin. Human SK-hep-1 cell line (derived from liver adenocarcinoma with oncogenic mesenchymal stem cells characteristics) (21) was cultured in DMEM supplemented with 10% FBS, 100 U/mL penicillin, 0.1 mg/mL streptomyc[1]in, 1 mM sodium pyruvate, and 1% nonessential amino acids.

In some experiments, HepG2 cells were treated with inhibitors of p38 (5 μM, SB203580, Cell Signaling Technology, Beverly, MA), NF-κB (10 μM, JSH-23, Sigma, St. Louis, MO, USA), JNK (5 μM, SP600125, Sigma, St. Louis, MO) or a combination of JSH-23 (10 μM) and SP600125 (5 μM) for 48 hours alone or with a combination of PHB1 silencing as described below.

For experiments with calyculin A (Santa Cruz Biotechnology Inc, Paso Robles, CA), 500 nM was added 30 minutes prior to the end of the experiment.

PHB1 silencing and overexpression in vitro

Cell lines were seeded in 6-well plates for *PHB1* overexpression or silencing. Huh7 and Hep3B cells ($2x10^5$) were forward transfected with 2 μg PHB1 overexpression or empty vector (Origene, Rockville, MD) for 48 hours using JetPRIME® reagent (Polyplus-transfection, Radnor, PA) according to manufacturer's instructions. For PHB1 silencing, pre-validated Silencer ® select siRNA against human *PHB1* (Ambion #S10424) or scramble siRNA control (Thermo Scientific) was reverse transfected into cells at dose of 20 nM in 6-well plates using LipoFectamine RNAiMAX transfection reagent (Invitrogen, Carlsbad, CA) for 24 to 72 hours. A second siRNA for *PHB1* (Ambion #S143790) was also tested at 50 nM.

RNA isolation and gene expression analysis

Total RNA was isolated using Trizol (Invitrogen). Gene expression was assessed using real-time PCR. Total RNA was subjected to reverse transcription using Moloney murine leukemia virus reverse transcriptase (Lucigen, Middleton, WI). TaqMan probes for human *PHB1, IL-8, PDGFA, MMP2, TGFB1* were purchased from ThermoFisher (Carlsbad, CA). The Universal PCR Master Mix were purchased from Bio-Rad (Hercules, CA). Hypoxanthine phosphoribosyltransferase 1 was used as a housekeeping gene. The thermal profile consisted of an initial denaturation at 95°C for three minutes followed by 40 cycles at 95°C for three seconds and at 60°C for 30 seconds. The cycle Ct value of the target genes was normalized to that of the housekeeping gene to obtain the delta Ct (ΔCt). The ΔCt was used to find the relative expression of target genes according to the formula: relative expression= $2^{-\Delta\Delta Ct}$, where ΔΔCt=ΔCt of target genes in experimental condition –ΔCt of target gene under control condition.

In some experiments HepG2 cells were first treated with PHB1 siRNA or scramble control for 48 hours, followed by actinomycin D (10 μg/ml, Sigma, St. Louis, MO) and *IL-8* mRNA levels were measured up to 8 hours after actinomycin D.

RNA-sequencing

RNA-sequencing and bioinformatics were provided by BGI Americas Corp (Cambridge, MA).

Protein isolation and western blot analysis

Nuclear extract isolation for cells was performed using the Nuclear Extraction kit (Abcam, Cambridge, MA), and total protein extracts from cells prepared using radioimmunoprecipitation assay (RIPA) lysis buffer (Abcam) containing protease and phosphatase inhibitor cocktail (ThermoFisher, Carlsbad, CA) was subjected to SDS-PAGE followed by western blotting according to standard methods (Amersham Biosciences, Waltham, MA). Membranes were probed with antibodies to PHB1 (Thermo Scientific, Waltham, MA, USA), IL-8 (Abcam, Cambridge, UK), phospho-JNK, JNK, phospho-ERK, ERK, phospho-p38 mitogen activated protein kinase (MAPK), p38 MAPK, c-JUN, TAK1 and phospho-TAK1, Phospho-IKKα/β (Ser176/180), Phospho-IκBα (Ser32), and IκBα (Cell Signaling Technology, Beverly, MA, USA), p65 (Protein Tech, Rosemont, IL). To ensure equal loading, membranes were probed with anti-actin or Histone H3 antibodies. For ECL chemiluminescence detection, the ChemiDoc™ XRS+ System (Bio-Rad, Hercules, CA) was used. Blots were quantified using the ImageJ densitometry program (National Institutes of Health), and test protein expression was normalized to actin (total protein extracts) or Histone H3 (nuclear extract) control.

Promoter constructs and luciferase assay

The human *IL-8* promoter (hIL-8-1450/+154) was purchased from Genecopoeia (Rockville, MD). The wild type (WT) human *IL-8* promoter -162/+44 (hIL-8 (-162/+44)-Luc) and hIL-8 (-162/+44)-Luc containing point mutations in the AP-1 and NF-κB DNA binding sites (ΔAP-1 hIL-8 (-162/+44)-Luc, ΔNF-κB hIL-8 (-162/+44)-Luc were kindly provided by Dr. Marc Hershenson (University of Michigan, Ann Arbor, Michigan, USA). For NF-κB (TGGGGACTTTCCGC)X5, AP-1 (TGACTAA)X7 reporter constructs, two complementary oligonucleotides containing the multimerzed elements were annealed and ligated into the *Bgl*II and *Sal*I restriction sites of the pLuc-Mcs plasmid using T4 DNA ligase (New England Biolabs, Ipswich, MA). The promoter constructs and pEZX/SV40 (1 μg) were co-transfected into

HepG2 cells with jetPRIME® following the manufacturer's instructions. Luciferase assays were performed 24 hours later using the Secrete-Pair Dual Luminescence Assay Kit (Genecopoeia) and the Dual Luciferase Reporter Assay System (Promega, Madison, WI) according to the manufacturer's protocol.

Chromatin immunoprecipitation (ChIP) and sequential-ChIP (Seq-ChIP) assay

To examine changes in protein binding to the AP-1 and NF-κB regions of the human *IL-8* promoter in an endogenous chromatin configuration following PHB1 knockdown, ChIP assays were done using the EpiTect ChIP OneDay protocol (Qiagen, Valencia, CA). Briefly, DNA was immunoprecipitated by c-JUN or p65 antibody. The final, purified DNA was detected by real time PCR analysis. PCR (186bp) of the human *IL-8* promoter region containing the AP-1 and NF-κB elements used forward primer 5'-AAGAAAACTTTCGTCATACTCCG-3' and reverse primer 5'-TGGCTTTTTATATCATCACCCTAC-3' (Gen-Bank accession no.NM_000584.3) (15).

In separate experiments, ChIP and Seq-ChIP were done using the manufacturer's suggested protocol from the Pierce agarose ChIP kit (ThermoFisher). Briefly, for AP-1, DNA was immunoprecipitated by anti-PHB1, anti-c-FOS and anti-c-JUN antibodies. For NF-κB, DNA was immunoprecipitated by anti-PHB1, anti-p65 and anti-p50 antibodies. The purified DNA was detected by PCR analysis. PCR of the human *IL-8* promoter region (GenBank® accession no. NM_000584) containing the AP-1 and NF-κB used forward primer 5'-ACTATATCTGTCACATGGTACTATG-3' (bp -230 to -255) and reverse primer 5'-CATTATGTCAGAGGAAATTCCACG-3' (-7 to -31 relative to TSS). All PCR products were run on 2% agarose gels. The PCR conditions consisted of an initial denaturation at 94°C for three minutes followed by 25 cycles at 94°C for 30 seconds, the annealing and extension at 67°C for 90 seconds using the Advantage GC 2 PCR kit (Clontech, Mountain View, CA), in accordance with their suggested protocol.

Total and mitochondrial ROS measurement

Total ROS levels were measured using the DCFDA kit (ab113851, Abcam) according to the manufacture's guide. Mitochondrial ROS were measured using MitoSOX™ Red mitochondrial superoxide indicator (M36008, Invitrogen). Cells were loaded with 5 μM MitoSOX in HBSS medium for 15 minutes at 37°C. After washing cells with warm PBS twice, fluorescence was measured by plate reader at excitation of 510 nm and emission of 580 nm. All the readings were normalized to live cell number.

Mitochondrial membrane potential measurement

Mitochondrial membrane potential was measured using the JC-1 assay kit (ab113850, Abcam). Cells were loaded with 5 μM JC-1 in DMEM medium for 30 minutes at 37°C. After washing cells with warm PBS twice, fluorescence was measured by plate reader at excitation of 488 nm and emission of 529 and 590 nm. All the readings were normalized to live cell number.

Cell viability measurement

Cell viability was measured using trypan blue (Invitrogen) staining.

Migration and invasion assays after treatment with conditioned media (CM)

To see the effect of released IL-8, HepG2 cells were first treated with PHB1 siRNA or scramble control for 48 hours in the presence of 10% FBS, CM (2 ml) was then used to treat parental HepG2 and SK-hep-1 cells for 24 hours with or without anti-IL-8 antibody (2.5 μg/ml, Abcam). The migration assay was measured using Culture-Insert 2 well in μ-Dish 35 mm kit from ibidi (Am Kloferspitz, Martinsried, Germany). Briefly, the cells were seeded onto the Culture-Insert of a 24-well plate. After 18 hours of plating the cells were treated with CM from PHB1 silenced-HepG2 cells or scrambled-HepG2 cells and incubated for 72 hours. After 24 hours, photographic images were acquired under an inverted microscope (EVOS XL core, Life technologies) and the migration occupied area was measured using the Image J software.

The invasion assay was assessed using Corning Matrigel Invasion Chamber kit (Bedford, MA, USA). Briefly, the cells were placed onto the top insert and treated with CM from PHB1 silenced-HepG2 cells or scrambled-HepG2 cells. Invaded cells on the bottom of the insert membrane were

stained with Diff-QuikTM stain. Invaded cells were counted by photographing the membrane through the microscope. For IL-8 blocking studies in the presence of CM (2 ml), cells were incubated for 24 or 72 hours with CM from PHB1 silenced-HepG2 cells in the presence of antibodies specific for IL-8 or control IgG and subsequently analyzed for the migration and invasiveness.

Statistical analysis

Data are expressed as mean ± standard error. Statistical analysis was performed using Student's T-test, ANOVA and Fisher's test. For mRNA and protein levels, ratios of genes and proteins to respective housekeeping densitometric values were compared. Since the HCC patieint samples are likely to be highly heterogeneous, we clustered the patients with the expression patterns of genes *PHB1* and *IL-8* using the Kmean algorithm in MATLAB (www.mathworks.com). The number of clusters is determined by the silhouette method. For survival analysis, log-rank test was used to compare the survival ratio differences between samples with high versus low *IL-8* expressions. Significance was defined by $p<0.05$.

ACKNOWLEDGEMENTS

This work was supported by NIH grant R01CA172086 (SC Lu, HP Yang, JM Mato), Plan Nacional of I+D SAF2017-88041-R and 777377-LITMUS-H2020-JTI-IMI2-2016-09, and CIBERehd MAT-3 and Severo Ochoa SEV-2016-0644 (to JM Mato). The funders had no role in study design, data collection and analysis, decision to publish, or preparation of the manuscript.

CONFLICT OF INTEREST

JMM is a consultant for Abbott; the other authors have nothing to declare.

AUTHOR CONTRIBUTIONS

JWY, BM, LBT, TL, HPY, WF, JW, YL – data acquisition, analysis, interpretation. JWY, BM and LBT wrote parts of the paper and prepared the figures

ZL – statistical analysis of human liver cancer specimens data

ES, JMM – critical reading of the manuscript, intellectual content

SCL - study concept and design, data analysis and interpretation, edited the manuscript, obtained funding and provided overall study supervision

REFERENCES

1. Nijtmans, L. G. J., Sanz, M. A., Grivell, L. A., and Coates, P. J. (2002) The mitochondrial PHB complex: roles in mitochondrial respiratory complex assembly, ageing and degenerative disease. *Cell Mol. Life Sci.* **59**, 143-155
2. Choi, D., Lee, S. J., Hong, S., Kim, I. H., and Kang, S. (2008) Prohibitin interacts with RNF2 and regulates E2F1 function via dual pathways. *Oncogene* **27**, 1716-1725
3. Wang, S., Fusaro, G., Padmanabhan, J., and Chellappan, S. P. (2002) Prohibitin co-localizes with Rb in the nucleus and recruits N-CoR and HDAC1 for transcriptional repression. *Oncogene* **21**, 8388-8396
4. Fusaro, G., Dasgupta, P., Rastogi, S., Joshi, B., and Chellappan, S. (2003) Prohibitin induces the transcriptional activity of p53 and is exported from the nucleus upon apoptotic signaling. *The Journal of Biological Chemistry* **278**, 47853-47861
5. McClung, J. K., Danner, D. B., Stewart, D. A., Smith, J. R., Schneider, E. L., Lumpkin, C. K., Dell'Orco, R. T., and Nuell, M. J. (1989) Isolation of a cDNA that hybrid selects antiproliferative mRNA from rat liver. *Biochem. and Biophys. Res. Commun*. **164**, 1316-1322
6. Rajalingam, K., Wunder, C., Brinkmann, V., Churin, Y., Hekman, M., Sievers, C., Rapp, U. R., and Rudel, T. (2005) Prohibitin is required for Ras-induced Raf-MEK-ERK activation and epithelial cell

migration. *Nat. Cell. Biol*. **7**, 837-843
7. Koushyar, S., Jiang, W. G., and Dart, D. A. (2015) Unveiling the potential of prohibitin in cancer. *Cancer Letters* **369**, 316-322
8. Liu, T., Tang, H., Lang, Y., Liu, M., and Li, X. (2009) MicroRNA-27a functions as an oncogene in gastric adenocarcinoma by targeting prohibitin. *Cancer Letters* **273**, 233-242
9. Kathiria, A. S., Neumann, W. L., Rhees, J., Hotchkiss, E., Cheng, Y., Genta, R. M., Meltzer, S. J, Souza, R. F., and Theiss, A. L. (2012) Prohibitin attenuates colitis-associated tumorigenesis in mice by modulating p53 and STAT3 apoptotic responses. *Cancer Res*. **72**, 5778-5789
10. Yang, H., Li, T. W. H., Zhou, Y., Peng, H., Liu, T., Zandi, E., Martínez-Chantar, M. L., Mato, J. M., and Lu, S. C. (2015) Activation of a novel c-Myc-miR27-Prohibitin 1 circuitry in cholestatic liver injury inhibits glutathione synthesis in mice. *Antioxidants & Redox Signaling* **22**, 259-274
11. Barbier-Torres, L., Beraza, N., Fernández-Tussy, P., Lopitz-Otsoa, F., Fernández-Ramos, D., Zubiete-Franco, I., Varela-Rey, M., Delgado, T. C., Gutiérrez, V., Anquita, J., Pares, A., Banales, J. M., Villa, E., Caballería, J., Alvarez, L., Lu, S. C., Mato, J. M., and Martínez-Chantar, M. L. (2015) Histone Deacetylase 4 promotes cholestatic liver injury in the absence of Prohibitin-1. *Hepatology* **62**, 1237-248
12. Ko, K. S., Tomasi, M. L., Iglesias-Ara, A., French, B. A., French, S. W., Ramani, K., Lozano, J. J., Oh, P., He, L., Stiles, B. L., Li, T. W., Yang, H., Martínez-Chantar, M. L., Mato, J. M., and Lu, S. C. (2010) Liver-specific deletion of prohibitin 1 results in spontaneous liver injury, fibrosis, and hepatocellular carcinoma in mice. *Hepatology* **52**, 2096-2108
13. Fan, W., Yang., H., Liu, T., Wang, J., Li, T. W., Mavila, N., Tang, Y., Yang, H., Peng, H., Tu, J., Annamalai, A., Noureddin, M., Krishnan, A., Gores, G. J., Martínez-Chantar, M. L., Mato, J. M., and Lu, S. C. (2017) Prohibitin 1 suppresses liver cancer tumorigenesis in mice and human hepatocellular and cholangiocarcinoma cells. *Hepatology* **65**, 1249-1266
14. Ramani, K., Mavila, N., Ko, K. S., Mato, J. M., and Lu, S. C. (2016) Prohibitin 1 Regulates the H19-Igf2 Axis and Proliferation in Hepatocytes. *The Journal of Biological Chemistry* **291**, 24148-24159
15. Jundi, K., and Greene, C. M. (2015) Transcription of Interleukin-8: How altered regulation can affect cystic fibrosis lung disease. *Biomolecules* **5**, 1386-1398
16. Gangwani, M. R., and Kumar, A. (2015) Multiple protein kinases via activation of transcription factors NF-κB, AP-1 and C/EBP-δ regulate the IL-6/IL-8 production by HIV-1 Vpr in astrocytes. *PloS One* **10**, e0135633
17. Bhattacharyya, S., Gutti, U., Mercado, J., Moore, C., Pollard, H. B., and Biswas, R. (2011) MAPK signaling pathways regulate IL-8 mRNA stability and IL-8 protein expression in cystic fibrosis lung epithelial cell lines. *Am. J. Physiol. Lung Cell and Mol. Physiol*. **300**, L81-87
18. Gui, T., Sun, Y., Shimokado, A., and Muragaki, Y. (2011) The roles of mitogen-activated protein kinase pathways in TGF-β-induced epithelial-mesenchymal transition. *J. Signal Transduct*. **2012**, 289243
19. Omori, E., Inagaki, M., Mishina, Y., Matsumoto, K., and Ninomiya-Tsuji, J. (2012) Epithelial transforming growth factor β-activated kinase 1 (TAK1) is activated through two independent mechanisms and regulates reactive oxygen species. *Proc. Natl. Acad. Sci. USA* **109**, 3365-3370
20. Fernando, R. I., Castillo, M. D., Litzinger, M., Hamilton, D. H., and Palena, C. (2011) IL-8 signaling plays a critical role in the epithelial-mesenchymal transition of human carcinoma cells. *Cancer Res*. **71**, 5296-5306
21. Eun, J. R., Jung, Y. J., Zhang, Y. L., Zhang, Y. H., Tschudy-Seney, B., Ramsamooj, R., Wan, Y. J., Theise, N. D., Zern, M. A., and Duan, Y. (2014) Hepatoma SK Hep-1 cells exhibit characteristics of oncogenic mesenchymal stem cells with highly metastatic capacity. *PLoS ONE* **9**, e110744.
22. Peng, Y. T., Chen, P., Ouyang, R. Y., and Song, L. (2015) Multifaceted role of prohibitin in cell survival and apoptosis. *Apoptosis* **20**, 1135-1149
23. Sato, S., Murata, A., Orihara, T., Shirakawa, T., Suenaga, K., Kigoshi, H., and Uesugi, M. (2011)

Marine natural product aurilide activates the OPA1-mediated apoptosis by binding to prohibitin. *Chem. Biol*. **18**, 131–139
24. Patel, N., Chatterjee, S. K., Vrbanac, V., Chung, I., Mu, C. J., Olsen, R. R., Waghorne, C., and Zetter, B. R. (2010) Rescue of paclitaxel sensitivity by repression of Prohibitin1 in drug-resistant cancer cells. *Proc Natl Acad Sci USA* **107**, 2503–2508
25. Jiang, L., Dong, P., Zhang, Z., Li, C., Li, Y., Liao, Y., Li, Z., Wu, Z., Guo, S., Mai, S., Xie, D., Liu, Z., Zhou, F. (2015) Akt phosphorylates Prohibitin 1 to mediate its mitochondrial localization and promote proliferation of bladder cancer cells. *Cell Death Dis*. **6**, e1660
26. Peng, X., Mehta, R., Wang, S., Chellappan, S., and Mehta, R. G. (2006) Prohibitin is a novel target gene of vitamin D involved in its antiproliferative action in breast cancer cells. *Cancer Res*. **66**, 7361–7369
27. Shi, S. L., Li, Q. F., Liu, Q. R., Xu, D. H., Tang, J., Liang, Y., Zhao, Z. L., and Yang, L. M. (2009) Nuclear matrix protein, prohibitin, was down-regulated and translocated from nucleus to cytoplasm during the differentiation of osteosarcoma MG-63 cells induced by ginsenoside Rg1, cinnamic acid, and tanshinone IIA (RCT). *J. Cell. Biochem*. **108**, 926–934
28. Gamble, S. C., Odontiadis, M., Waxman, J., Westbrook, J. A., Dunn, M. J., Wait, R., Lam, E. W., and Bevan, V. L. (2004) Androgens target prohibitin to regulate proliferation of prostate cancer cells. *Oncogene* **23**, 2996–3004
29. Guan, X., Liu, Z., Wang, L., Johnson, D. G., and Wei, Q. (2014) Identification of prohibitin and prohibiton as novel factors binding to the p53 induced gene 3 (PIG3) promoter (TGYCC)(15) motif. *Biochem. Biophys. Res. Commun*. **443**, 1239–1244
30. Liu, T., Yang, H., Fan, W., Tu, J., Li, T. W. H., Wang, J., Shen, H., Yang, H., Xiong, T., Steggerda, J., Liu, Z., Noureddin, M., Maldondo, S. S, Annamalai, A., Seki, E., Mato, J. M., and Lu, S. C. (2018) Mechanisms of MAFG dysregulation in cholestatic liver injury and development of liver cancer. *Gastroenterology* 10.1053/j.gastro.2018.04.032
31. Mantovani, A., Savino, B., Locati, M., Zammataro, L., Allavena, P., and Bonecchi, R. (2010) The chemokine system in cancer biology and therapy. *Cytokine Growth Factor Rev*. **21**, 27–39
32. Xie, K. (2001) Interleukin-8 and human cancer biology. *Cytokine Growth Factor Rev*. **12**, 375-391
33. Joyce, J. A., and Pollard, J. W. (2009) Microenvironmental regulation of metastasis. *Nat. Rev. Cancer* **9**, 239-252
34. Huang, W., Chen, Z., Zhang, L., Tian, D., Wang, D., Fan, D., Wu, K., and Xia, L. (2015) Interleukin-8 induces expression of FOXC1 to promote transactivation of CXCR1 and CCL2 in hepatocellular carcinoma cell lines and formation of metastases in mice. *Gastroenterology* **149**, 1053-1067
35. Ren, Y., Poon, R. T. P., Tsui, H. T, Chen, W. H., Li, Z., Lau, C., Yu, W. C., and Fan, S. T. (2003) Interleukin-8 serum levels in patients with hepatocellular carcinoma correlations with clinicopathological features and prognosis. *Clinical Cancer Research* **9**, 5996-6001
36. Krause, A., Holtmann. H., Eickemeier, S., Winzen, R., Szamel, M., Resch, K., Saklatvala, J., and Kracht, M. (1998) Stress-activated protein kinase/Jun N-terminal kinase is required for interleukin (IL)-1-induced IL-6 and IL-8 gene expression in the human epidermal carcinoma cell line KB. *J. Biol. Chem.* **273**, 23681–23689
37. Theiss, A. L., Jenkins, A. K., Okoro, N. I., Klapproth, J. M. A., Merlin, D., and Sitaraman, S. V. (2009) Prohibitin inhibits tumor necrosis factor alpha–induced nuclear factor-kappa B nuclear translocation via the novel mechanism of decreasing importin α3 expression. *Mol. Biol. Cell*. **20**, 4412–4423
38. Rajalingam, K., Wunder, C., Brinkmann, V., Churin, Y., Hekman, M., Sievers, C., Rapp, U. R., and Rudel, T. (2005) Prohibitin is required for Ras-induced Raf-MEK-ERK activation and epithelial cell migration. *Nat. Cell Biol*. **7**, 837-843
39. Chowdhury, I., Thompson, W. E., Welch, C., Thomas, K., and Matthews, R. (2013) Prohibitin (PHB) inhibits apoptosis in rat granulosa cells (GCs) through the extracellular signal-regulated kinase 1/2 (ERK1/2) and the Bcl family of proteins. *Apoptosis* **18**, 1513-1525

40. Liu, Y., Du, Y., Wang, H., Du, L., and Feng, W. H. (2017) Porcine reproductive and respiratory syndrome virus (PRRSV) up-regulates IL-8 expression through TAK-1/JNK/AP-1 pathways. *Virology* **506**, 64-72
41. Waugh, D. J. J., and Wilson, C. (2008) The interleukin-8 pathway in cancer. *Clinical Cancer Research* **14**, 6735-6741
42. Anaya, J., Reon, B., Chen, W. M., Bekiranov, S., and Dutta, A. (2016) A pan-cancer analysis of prognostic genes. *PeerJ* **3**, e1499
43. Anaya, J. (2016) OncoLnc: linking TCGA survival data to mRNAs, miRNAs, and lncRNAs. *PeerJ Computer Science* **2**, e67. https://doi.org/10.7717/peerj-cs.67

ABBREVIATIONS USED (alphabetical order):
CCA, cholangiocarcinoma; **ChIP**, Chromatin immunoprecipitation; **CM,** conditioned media; **FBS**, fetal bovine serum; **HCC**, hepatocellular carcinoma; **IGF-2,** insulin-like growth factor 2; **IL-8,** interleukin-8; **KO**, knockout; **MMP2,** matrix metalloproteinase-2; **NT,** non-tumorous tissue; **PCR**, polymerase chain reaction; **PDGFA,** platelet-derived growth factor subunit A; **PHB1**, prohibitin 1; **Rb**, retinoblastoma protein; **ROS,** reactive oxygen species; **Seq-ChIP,** sequential-ChIP; **siRNA**, small interfering RNA; **TGFB1,** transforming growth factor beta-1; **WT,** wild type

FIGURE LEGENDS

Figure 1. PHB1 silencing upregulates cancer related genes in liver and colon cancer cells. (**A**) Top 20 DEGs enriched pathways in PHB1-silenced HepG2 cells analyzed by RNA-Seq. (**B**) Soluble mediator genes secreted by tumor cells (*IL-8*, *PDGFA*, *MMP-2* and *TGFB1*) in the KEGG set Pathway in cancer were > 2-fold upregulated in PHB1-silenced HepG2 cells. (**C**) qRT-PCR analysis for soluble mediator genes secreted by tumor cells (*IL-8*, *PDGFA*, *MMP-2* and *TGFB1*) in PHB1-silenced HepG2 cells. (**D**) *IL-8* mRNA expression in PHB1-silenced HCC cells (HepG2 and Huh7), Mz-ChA-1 cells (CCA cell line) and HCT116 cells (colorectal carcinoma cell line). $^{**}P < 0.01$ versus respective controls.

Figure 2. PHB1 and IL-8 expression in HCC. (**A**) *PHB1* and *IL-8* mRNA levels in human HCC and adjacent non-tumoral tissues (n=178). (**B**) HCC samples clustered with the Kmeans algorithm: Cluster I with elevated *PHB1* and lower *IL-8* expression (n=58); Cluster II with reduced *PHB1* expression (n=91) and Cluster III with higher *PHB1* and *IL-8* expressions (n=29). (**C**) Pearson correlation analysis between *PHB1* and *IL-8* in Cluster II. (**D**) *IL-8* mRNA levels in HCC compared to adjacent non-tumoral tissue in GEO databases GSE54236 (adjacent n=80, HCC n=81) and GSE36376 (adjacent n=82, HCC n=102). (**E**) Survival of patients with HCC from the TCGA dataset, classified into *IL-8* high tumors (upper 33th percentile, n=118) or *IL-8* low tumors (lower 33th percentile, n=118).

Figure 3. PHB1 negatively regulates IL-8 expression. (**A**) Western blot analysis of intracellular and secreted IL-8 in PHB1 silenced HepG2, Huh7 and Hep3B cells. (**B**) *IL-8* mRNA expression and (**C**) western blot analysis of intracellular and secreted IL-8 in PHB1 overexpressing Huh7 and Hep3B cells. All densitometric values were normalized to β-Actin. Results are expressed as mean ± standard error of the mean from at least three independent experiments. $^{*}P < 0.05$, $^{**}P < 0.01$ versus SC; $^{\#}P < 0.05$, $^{\#\#}P < 0.01$ versus respective controls. Abbreviations: SC, scramble siRNA; PHB1 si, PHB1 siRNA; EV, empty vector; PHB1 OE, PHB1 overexpression vector.

Figure 4. JNK and NF-κB signaling pathways are required for PHB1 silencing-induced IL-8 expression. (**A**) Effect of actinomycin D (Act D) treatment on *IL-8* mRNA levels in PHB1-silenced HepG2 cells. (**B**) Western blot analysis of total and phosphorylated JNK, p38 and ERK in PHB1-silenced HepG2 cells. All densitometric values were normalized to β-Actin. (**C**) *PHB1* and *IL-8* mRNA expression in PHB1-silenced HepG2 cells after the inhibition of either NF-κB or JNK alone or combined. HepG2 cells were transfected with a negative control or PHB1 siRNA for 24 hours followed by the treatment with inhibitors of NF-κB (JSH) or JNK (SP) individually or combined for another 48 hours. Results are expressed as mean ± standard error of the mean from at least three independent experiments. $^{**}P < 0.01$ versus respective SC controls; $^{\#\#}P < 0.01$ versus PHB1 si vehicle and $^{\dagger}P < 0.05$ versus PHB1 si SP. Abbreviations: SC, scramble siRNA; PHB1 si, PHB1 siRNA; JSH, JSH-23; SP, SP60125.

Figure 5. PHB1 silencing-induced *IL-8* promoter activity requires NF-κB and AP-1. (**A**) Promoter activity of NF-κB- and AP-1-driven luciferase reporter constructs after PHB1 knockdown. Results are expressed as mean ± standard error of the mean from at least three independent experiments. $^{*}P < 0.05$, $^{**}P < 0.01$ versus SC. (**B**) Effects of NF-κB and AP-1 sites mutations on PHB1 silencing-induced transcription from the *IL-8* promoter. HepG2 cells were transfected with PHB1 siRNA and effects on *IL-8* promoter (1450/+154) activity or reporter activities driven by human *IL-8* promoter (162/+44) that is WT or mutated in the AP-1 or NF-κB elements were measured. $^{**}P < 0.01$ versus respective controls, $\#\#P < 0.01$, versus SC of WT *IL-8* promoter. (**C**) Western blots of c-Jun and p65 in nuclear extracts from PHB1 knockdown HepG2 cells. All densitometric values were normalized to Histone H3. (**D**) Effects of PHB1 knockdown on p65 and c-Jun binding to regions of the *IL-8* promoter measured by ChIP–qPCR. Results are expressed as mean ± standard error of the mean from at least three independent experiments. $^{**}P < 0.01$

versus respective controls. Abbreviations: SC, scramble siRNA; PHB1 si, PHB1 siRNA. (**E**) Western blots of the NF-κB signaling pathway upon PHB1 knockdown. PHB1 was knocked down between 24 and 72 hours in HepG2 cells and Phospho-IKKα/β (Ser176/180), Phospho-IκBα (Ser32), and IκBα were blotted. All densitometric values were normalized to Actin. $^{**}P < 0.01$ versus respective SC control.

Figure 6. PHB1 binds to the *IL-8* promoter in the presence of c-JUN, but not c-FOS, p50 or p65. (**A**) IL-8 promoter region containing the AP-1 and NF-κB sites are shown, as well as the region covered by the primers. HepG2 cells were used for ChIP and Seq-ChIP assays as described in Methods. (**B**) PHB1 does not bind directly on ChIP assay to the *IL-8* promoter spanning the region shown in (**A**). PHB1 does not bind to the IL-8 promoter in the presence of p50 (**C**), p65 (**D**), c-FOS (**E**) but it binds in the presence of c-JUN (**F**).

Figure 7. PHB1 knockdown-induced IL-8 secretion promotes migration and invasion of cancer cells. Migration analysis in (**A**) HepG2 and (**B**) SK-hep-1 cells treated with conditioned medium (CM) obtained from HepG2 cells transfected with SC or PHB1 siRNA in the presence of IL-8 antibody or IgG as a negative control. (**C**) Invasion assay with the same conditions as in B. Results are expressed as mean ± standard error of the mean from at least three independent experiments. $^{**}P < 0.01$ versus SC-CM.; $^{\#\#}P < 0.01$, versus PHB1 si-CM. Abbreviations: SC, scramble siRNA; PHB1 si, PHB1 siRNA; SC-CM, conditioned medium obtained from HepG2 transfected with SC; PHB1 si-CM, conditioned medium obtained from HepG2 transfected with PHB1 siRNA; IgG: Immunoglobulin G; IL-8 Ab, interleukin-8 antibody.

A

Top 20 Statistics of Pathway Enrichment

#	Pathway	DEGs with pathway annotation (1651)	Pvalue
1	DNA replication	26 (1.57%)	4.95E-16
2	Cell cycle	50 (3.03%)	4.45E-12
3	p53 signaling pathway	37 (2.24%)	1.32E-08
4	HTLV-I infection	65 (3.94%)	1.81E-06
5	Mismatch repair	13 (0.79%)	2.95E-05
6	Complement and coagulation cascades	33 (2%)	2.19E-04
7	Homologous recombination	12 (0.73%)	3.21E-04
8	**Pathways in cancer**	**75 (4.54%)**	**3.81E-04**
9	Base excision repair	13 (0.79%)	6.51E-04
10	Nucleotide excision repair	16 (0.97%)	9.12E-04
11	PPAR signaling pathway	25 (1.51%)	9.58E-04
12	Osteoclast differentiation	35 (2.12%)	1.06E-03
13	Bladder cancer	15 (0.91%)	1.64E-03
14	Fanconi anemia pathway	16 (0.97%)	1.69E-03
15	Oocyte meiosis	32 (1.94%)	1.74E-03
16	Ascorbate and aldarate metabolism	9 (0.55%)	1.89E-03
17	Malaria	16 (0.97%)	1.95E-03
18	Axon guidance	44 (2.67%)	4.60E-03
19	One carbon pool by folate	8 (0.48%)	4.75E-03
20	Pyrimidine metabolism	24 (1.45%)	5.03E-03

B

Up-regulated genes in Pathways in cancer

Genes	Proteins	Fold change
IL-8	Interleukin-8	**16.00**
PDGFA	Platelet-derived growth factor subunit A	**8.00**
MMP2	Matrix metalloproteinase-2	**5.66**
TGFB1	Transforming growth factor beta-1	**2.44**

C

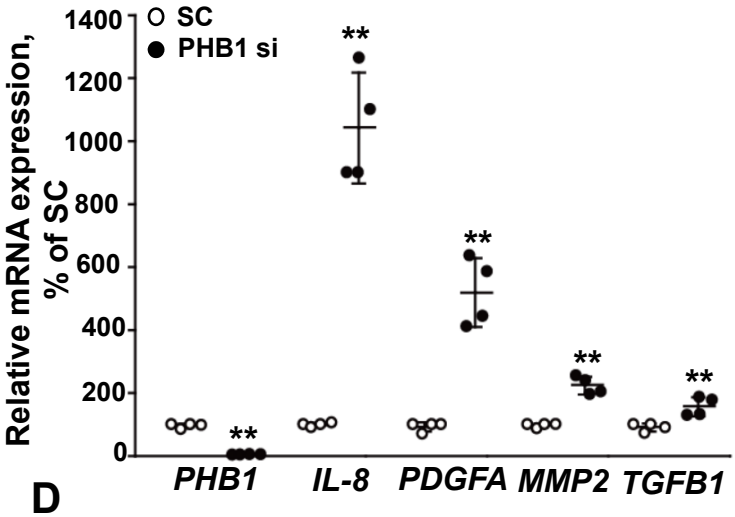

D

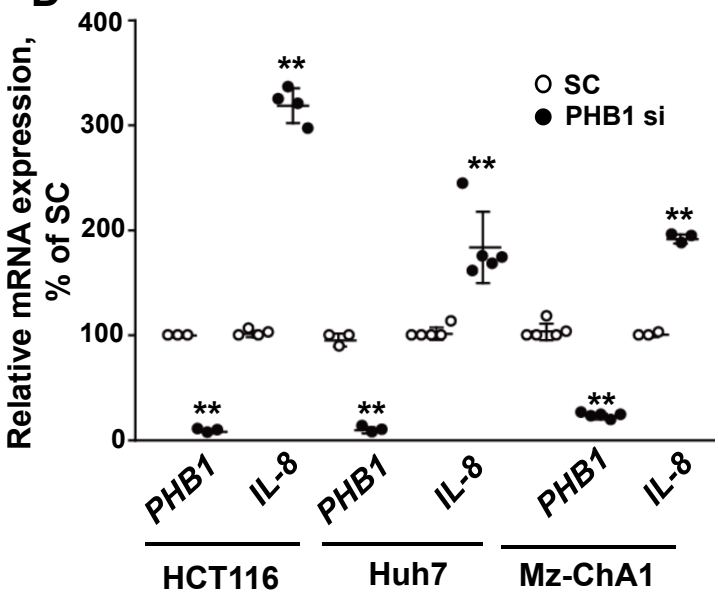

Figure 1

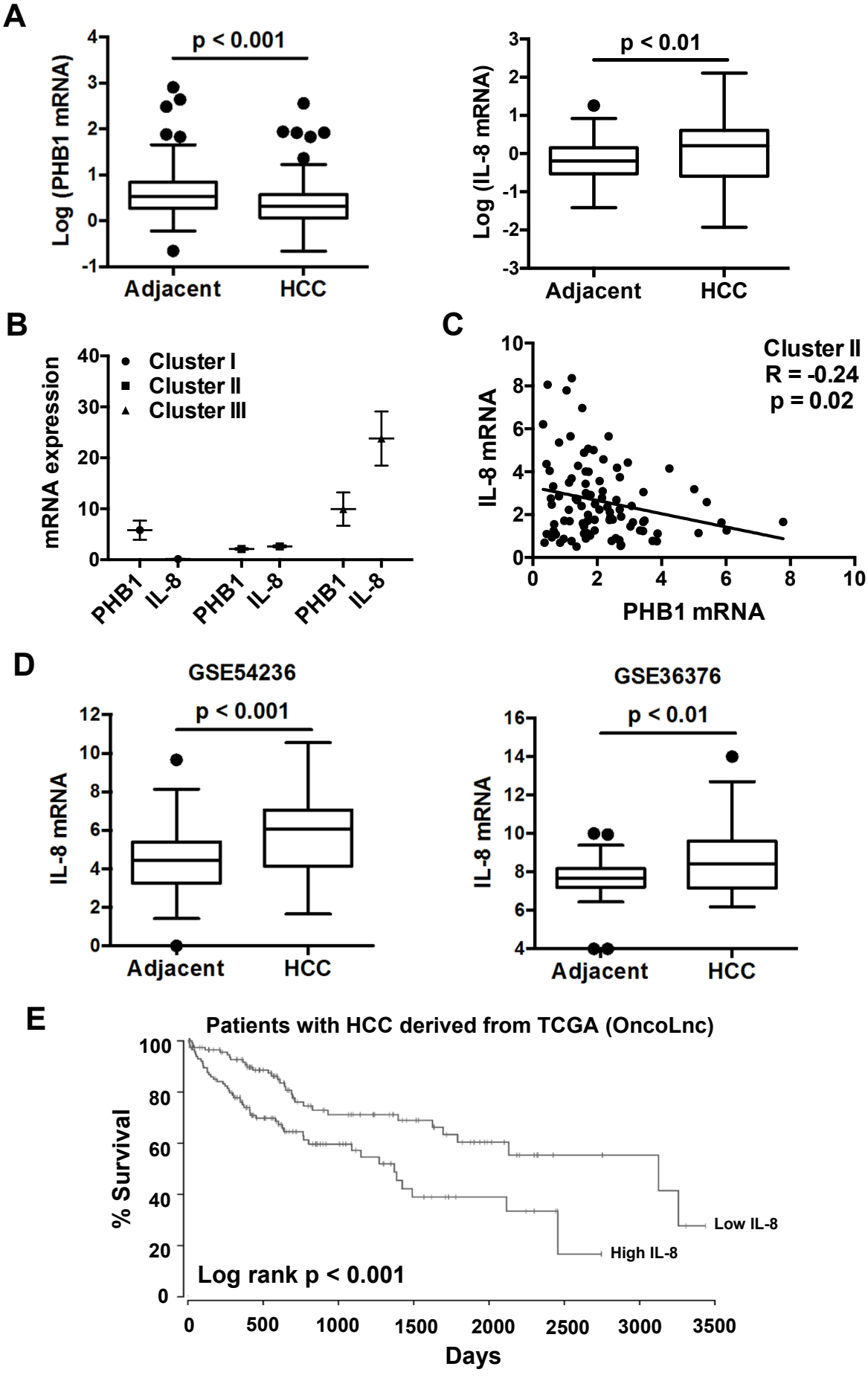
A
p < 0.001
Log (PHB1 mRNA)
Adjacent
HCC
p < 0.01
Log (IL-8 mRNA)
Adjacent
HCC
B
Cluster I
Cluster II
Cluster III
mRNA expression
PHB1
IL-8
PHB1
IL-8
PHB1
IL-8
C
Cluster II
R = -0.24
p = 0.02
IL-8 mRNA
PHB1 mRNA
D
GSE54236
p < 0.001
IL-8 mRNA
Adjacent
HCC
GSE36376
p < 0.01
IL-8 mRNA
Adjacent
HCC
E
Patients with HCC derived from TCGA (OncoLnc)
% Survival
Low IL-8
High IL-8
Log rank p < 0.001
Days

Figure 2

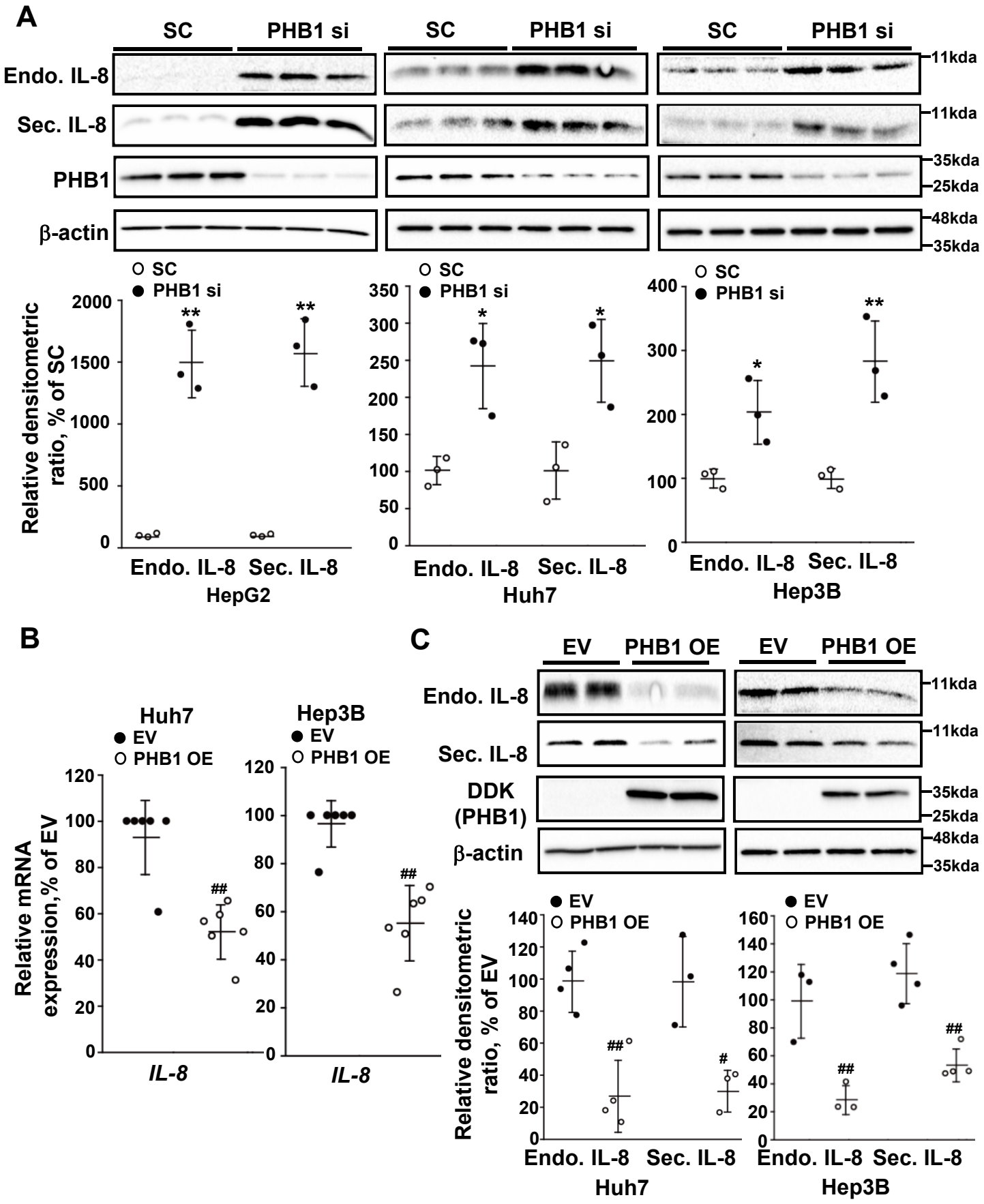
A
SC
PHB1 si
Endo. IL-8
Sec. IL-8
PHB1
β-actin
11kda
35kda
25kda
48kda
Relative densitometric ratio, % of SC
HepG2
Huh7
Hep3B
B
Huh7
Hep3B
EV
PHB1 OE
Relative mRNA expression,% of EV
IL-8
C
DDK (PHB1)
Relative densitometric ratio, % of EV

Figure 3

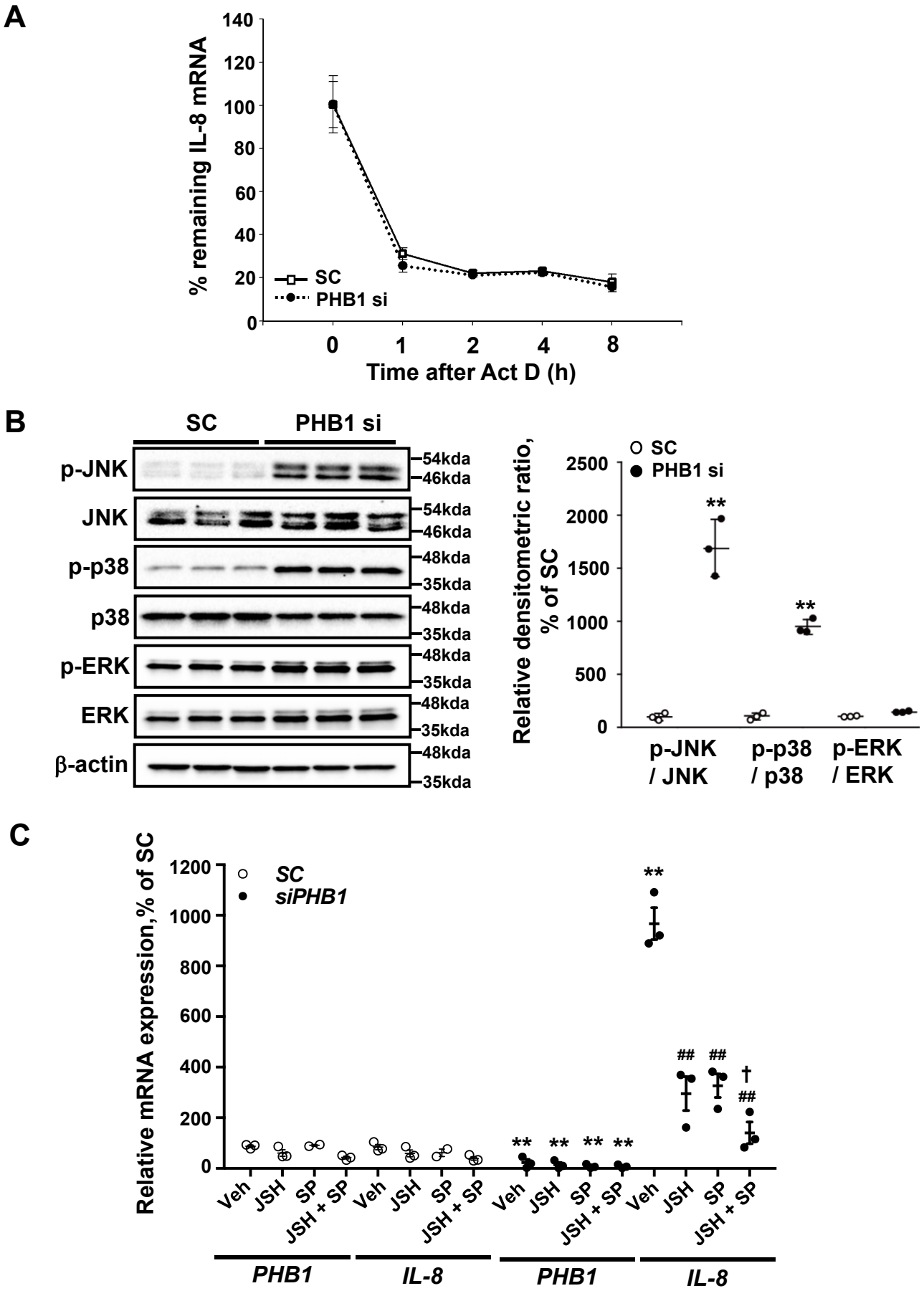
A
% remaining IL-8 mRNA
140
120
100
80
60
40
20
0
SC
PHB1 si
0
1
2
4
8
Time after Act D (h)
B
SC
PHB1 si
p-JNK
JNK
p-p38
p38
p-ERK
ERK
β-actin
54kda
46kda
48kda
35kda
Relative densitometric ratio, % of SC
2500
2000
1500
1000
500
0
**
p-JNK / JNK
p-p38 / p38
p-ERK / ERK
C
Relative mRNA expression,% of SC
SC
siPHB1
1200
1000
800
600
400
200
0
**
##
†
Veh
JSH
SP
JSH + SP
PHB1
IL-8

Figure 4

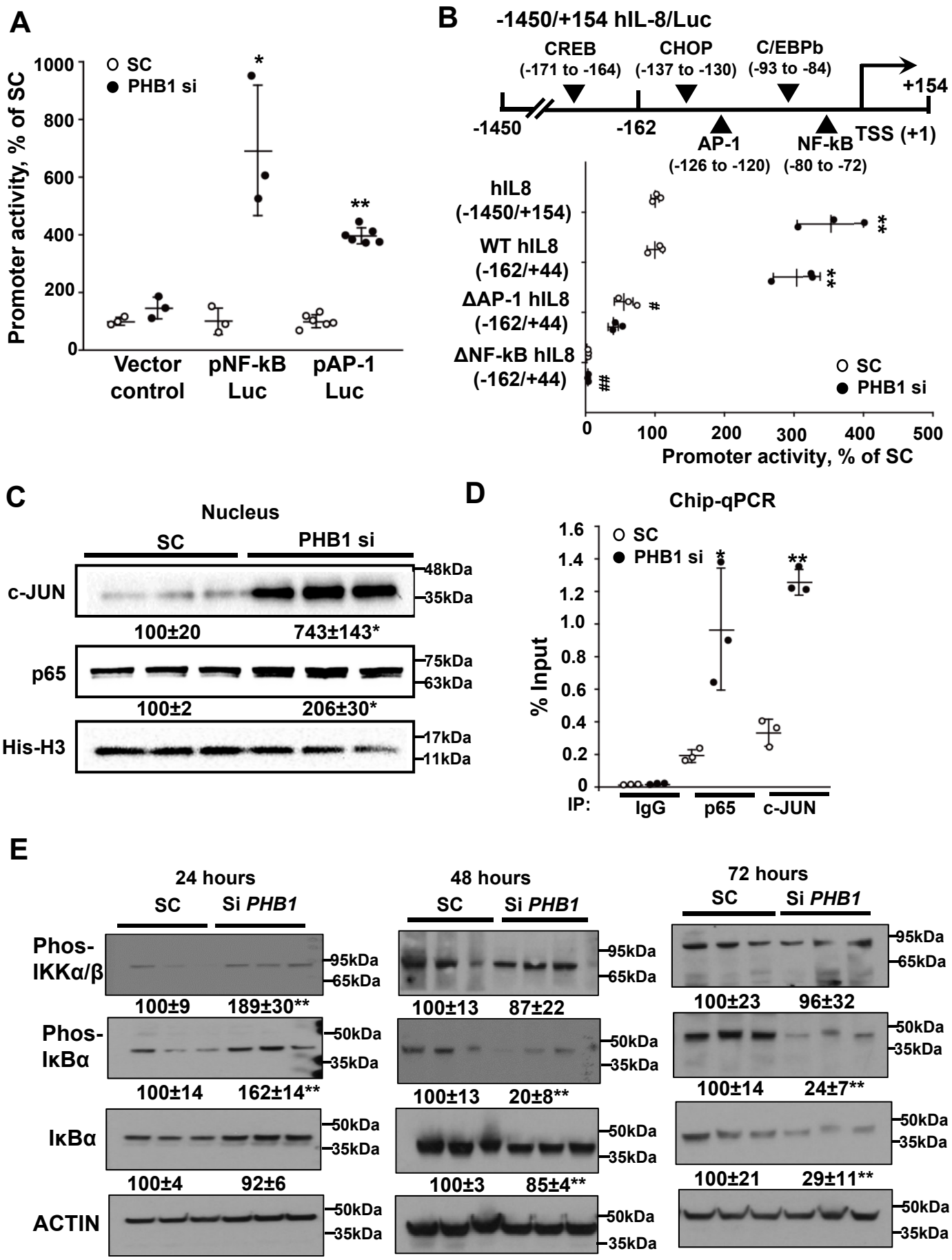
A
SC
PHB1 si
Promoter activity, % of SC
1000
800
600
400
200
0
Vector control
pNF-kB Luc
pAP-1 Luc
B
-1450/+154 hIL-8/Luc
CREB (-171 to -164)
CHOP (-137 to -130)
C/EBPb (-93 to -84)
+154
-1450
-162
AP-1 (-126 to -120)
NF-kB (-80 to -72)
TSS (+1)
hIL8 (-1450/+154)
WT hIL8 (-162/+44)
ΔAP-1 hIL8 (-162/+44)
ΔNF-kB hIL8 (-162/+44)
SC
PHB1 si
0
100
200
300
400
500
Promoter activity, % of SC
C
Nucleus
SC
PHB1 si
c-JUN
48kDa
35kDa
100±20
743±143*
p65
75kDa
63kDa
100±2
206±30*
His-H3
17kDa
11kDa
D
Chip-qPCR
SC
PHB1 si
% Input
1.6
1.4
1.2
1.0
0.8
0.6
0.4
0.2
0
IP:
IgG
p65
c-JUN
E
24 hours
48 hours
72 hours
SC
Si PHB1
Phos-IKKα/β
95kDa
65kDa
100±9
189±30**
100±13
87±22
100±23
96±32
Phos-IκBα
50kDa
35kDa
100±14
162±14**
100±13
20±8**
100±14
24±7**
IκBα
50kDa
35kDa
100±4
92±6
100±3
85±4**
100±21
29±11**
ACTIN
50kDa
35kDa

Figure 5

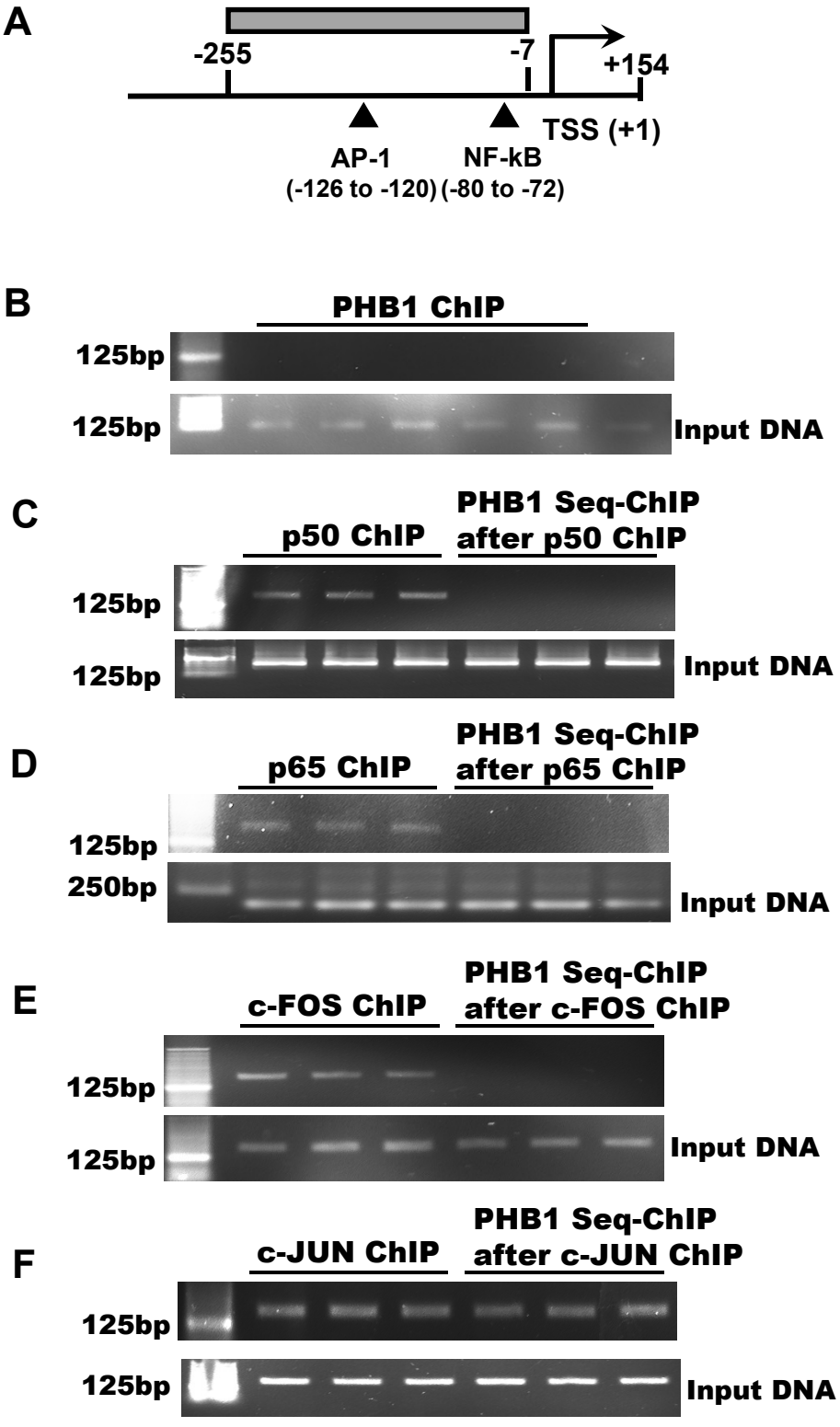
A
-255
-7
+154
TSS (+1)
AP-1
(-126 to -120)
NF-kB
(-80 to -72)
B
PHB1 ChIP
125bp
125bp
Input DNA
C
p50 ChIP
PHB1 Seq-ChIP
after p50 ChIP
125bp
125bp
Input DNA
D
p65 ChIP
PHB1 Seq-ChIP
after p65 ChIP
125bp
250bp
Input DNA
E
c-FOS ChIP
PHB1 Seq-ChIP
after c-FOS ChIP
125bp
125bp
Input DNA
F
c-JUN ChIP
PHB1 Seq-ChIP
after c-JUN ChIP
125bp
125bp
Input DNA

Figure 6

A

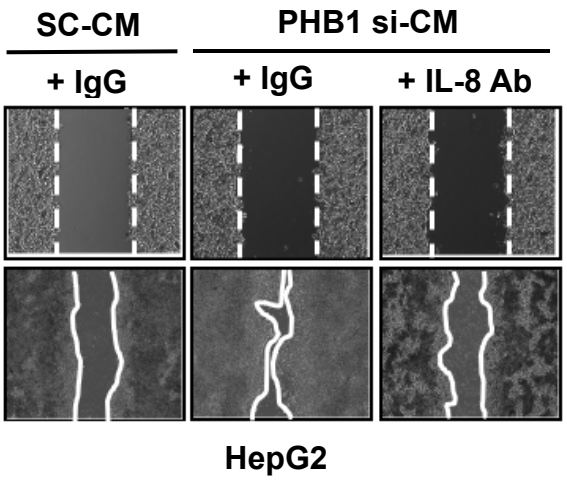
SC-CM
PHB1 si-CM
+ IgG
+ IgG
+ IL-8 Ab
HepG2

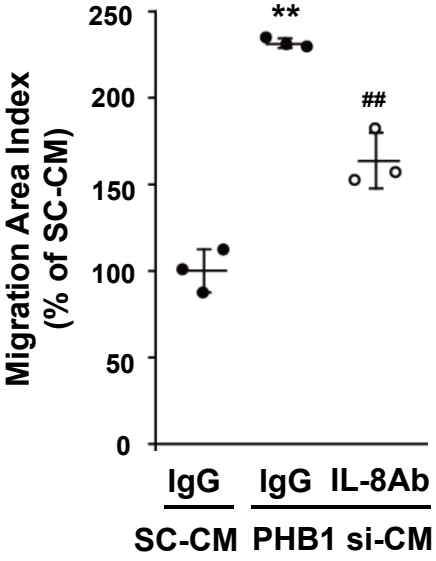
Migration Area Index
(% of SC-CM)
250
200
150
100
50
0
**
##
IgG
IgG
IL-8Ab
SC-CM
PHB1 si-CM

B

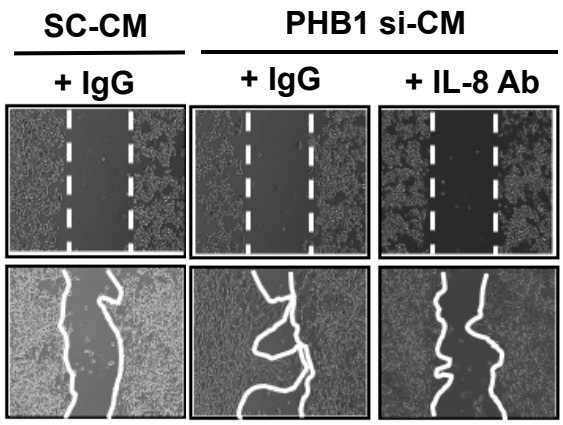
SC-CM
PHB1 si-CM
+ IgG
+ IgG
+ IL-8 Ab
SK-hep1

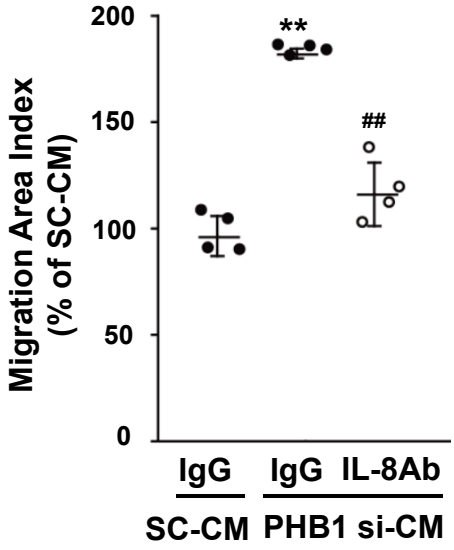
Migration Area Index
(% of SC-CM)
200
150
100
50
0
**
##
IgG
IgG
IL-8Ab
SC-CM
PHB1 si-CM

C

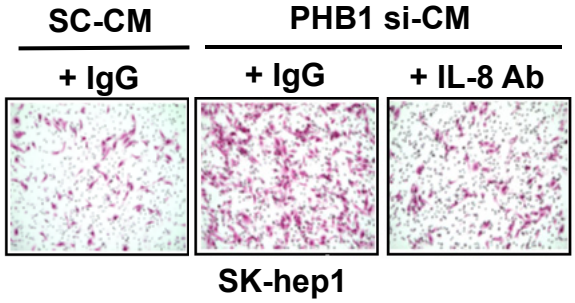
SC-CM
PHB1 si-CM
+ IgG
+ IgG
+ IL-8 Ab
SK-hep1

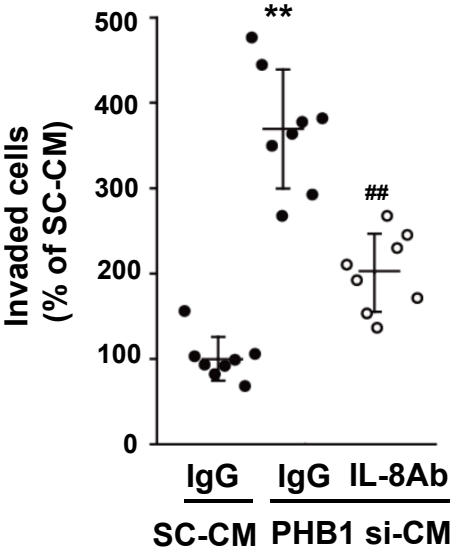
Invaded cells
(% of SC-CM)
500
400
300
200
100
0
**
##
IgG
IgG
IL-8Ab
SC-CM
PHB1 si-CM

Figure 7